Mechanical Properties, Morphology, and Crystallization Behavior of New Thermoplastic Polyimide (N-TPI)/Poly(ether sulfone) Blends

MITSUHIRO SHIBATA, KOICHI OZAWA, RYUTOKU YOSOMIYA

Department of Industrial Chemistry, Chiba Institute of Technology, 2-17-1, Tsudanuma, Narashino, Chiba 275-0016, Japan

Received 7 November 2000; accepted 7 May 2001

ABSTRACT: Blends of wholly aromatic new thermoplastic polyimide (N-TPI) and poly(ether sulfone) (PES) were prepared by melt-mixing and subsequent injection molding. Their mechanical properties, morphology, and crystallization behavior were investigated. A synergistic effect on the flexural properties was observed for the N-TPI/PES blends over the whole compositions. Differential scanning calorimetric analysis confirmed that the blend is an immiscible system and that the crystallinity of the N-TPI component is very low (0.4–1.4%) irrespective of the composition. Scanning electron microscopic analysis suggested that the improvement in flexural properties is likely due to the reinforcement of the PES matrix by the fibrous N-TPI phase for the N-TPI/PES (40/60, 20/80) blends. For N-TPI/PES (80/20, 60/40), the orientation of the matrix N-TPI rather than the fibrillation of the PES phase along the melt-flow direction may contribute to the synergism observed. Also, study of the isothermal crystallization behavior of the blends revealed that the addition of 10 wt % PES accelerates the crystallization of N-TPI and further addition causes the retardation of it. © 2002 John Wiley & Sons, Inc. J Appl Polym Sci 83: 1366–1374, 2002

Key words: all aromatic new thermoplastic polyimide; poly(ether sulfones); blends; mechanical properties, synergistic effect

INTRODUCTION

Polymer blends of different kinds of wholly aromatic thermoplastic polymers have received considerable attention, mainly in view of the attainment of more balanced mechanical properties, processability, and solvent resistance without affecting the superior heat resistance. Recently, a new wholly aromatic thermoplastic polyimide [N-TPI, Mitsui–Toatsu Chemicals Inc. (now Mitsui Chemical Co.)] was synthesized from 4,4′-bis(3,3′-aminophenoxy)biphenyl and pyromellitic dianhydride.[1] The polyimide is a semicrystalline polymer with a glass transition temperature (T_g) of 250°C and a melting point (T_m) of 380°C.[2–5] In terms of its superior mechanical properties, high-temperature stability, solvent resistance, and melt processability, N-TPI is a very promising material. Blends of N-TPI with other engineering plastics such as polyetherimide (PEI, Ultem)[6] and poly(aryl ether ketone)s[7,8] were studied by several workers.

In the present work, the mechanical properties of the blends of N-TPI with poly(ether sulfone) (PES) as another wholly aromatic thermoplastic polymer were investigated. It was found that the N-TPI/PES blends show synergism of the me-

Correspondence to: M. Shibata (shibata@pf.it-chiba.ac.jp).

Journal of Applied Polymer Science, Vol. 83, 1366–1374 (2002)

DOI 10.1002/app.10016

chanical properties. Recently, polymer blends exhibiting a synergistic effect on the mechanical properties and processability have been paid considerable attention. Most of the reported blends exhibiting remarkable synergism are those containing liquid crystalline polymer (LCP) where the orientation of LCP fibrils occurs.[9–12] The appearance of synergism for blends without LCP is very interesting. The crystallinity, miscibility, and morphologies of the N-TPI/PES blends were investigated in connection with the mechanical properties. Also, the isothermal crystallization behavior of N-TPI in blends with PES was investigated.

EXPERIMENTAL

Materials

N-TPI with a weight-average molecular weight (M_w) of about 30,000 and PES (Grade E2010) were kindly supplied by Mitsui–Toatsu Chemicals, Inc.

Sample Preparation

The polymers were dried at 100°C in a vacuum oven for at least 5 h before use. Blending of N-TPI and PES was performed using a Laboplasto-Mill with a twin-rotary mixer (Toyo Seiki Co. Ltd., Japan). The molten mixing was carried out at 400°C, the rotary speed was 50 rpm, and the mixing time was 5 min. The obtained blends were cut into the small pieces and again dried at 100°C in a vacuum oven before injection molding. The weight ratios of N-TPI/PES were 100/0, 90/10, 80/20, 70/30, 60/40, 40/60, 20/80, and 0/100. Dumbbell specimens (width 5 mm × thickness 2 mm × length of parallel part 32 mm × total length 72 mm) were molded using a desk injection-molding machine (Little-Ace I Type, Tsubako Co. Ltd., Japan). The cylinder temperature and the molding temperature during the injection molding were 430 and 120°C, respectively.

Measurements

Differential scanning calorimetry (DSC) was performed on a Perkin–Elmer DSC Pyris 1 DSC in a nitrogen atmosphere. To eliminate the influence of the thermal history, after the samples were heated to 410°C and held at that temperature for 5 min, DSC thermograms were monitored between 410 and 50°C at a cooling rate of 120°C/min, and then the second heating scans were also monitored between 50 and 410°C at a heating rate of 20°C/min for determining the glass transition temperature (T_g) and melting temperature (T_m). The T_g was obtained as the midpoint of the heat-capacity change. The samples for isothermal crystallization were heated to 420°C at a rate of 100°C/min, held at this temperature for 5 min, and then cooled to the appropriate crystallization temperature (T_c) 315–330°C at the rate of 120°C/min. The heat generated during the development of the crystalline phase was recorded until no further heat evolution was observed and then was analyzed according to the usual procedure to obtain the relative degree of crystallinity. The relative degree of crystallinity, as a function of time, was found from eq. (1):

$$\chi_c(t)/\chi_c(\infty) = \int_{t_0}^{t} (dH/dt)\, dt \Big/ \int_{t_0}^{\infty} (dH/dt)\, dt \quad (1)$$

where t_0 is the time at which the sample attains isothermal conditions, as indicated by a flat baseline after the initial spike in the thermal curve; $\chi_c(t)$, the degree of crystallinity at time t; $\chi_c(\infty)$, the ultimate crystallinity at a very long time; and dH/dt, the heat-flow rate. At the end of each isothermal experiment, the samples were reheated at a heating rate of 20°C/min, for measuring the melting temperature.

Flexural tests were performed using an Autograph AGS-500C (Shimazu Co. Ltd., Japan) based on the standard method for testing the flexural properties of rigid plastics [JIS K7203 (1982)]. The span length was 30 mm, and the testing speed was 10 mm/min.

The morphology of the blends was observed by scanning electron microscopy (SEM), using a JSM-6300 machine (Japan Electron Co., Japan). All samples were fractured in directions perpendicular and parallel to the melt-flow direction after immersion in liquid nitrogen for about 5 min. The fracture surfaces were sputter-coated with gold to provide enhanced conductivity.

RESULTS AND DISCUSSION

Mechanical Properties and Morphologies of N-TPI/PES Blends

The flexural mechanical properties of the injection-molded N-TPI/PES blends measured by load-

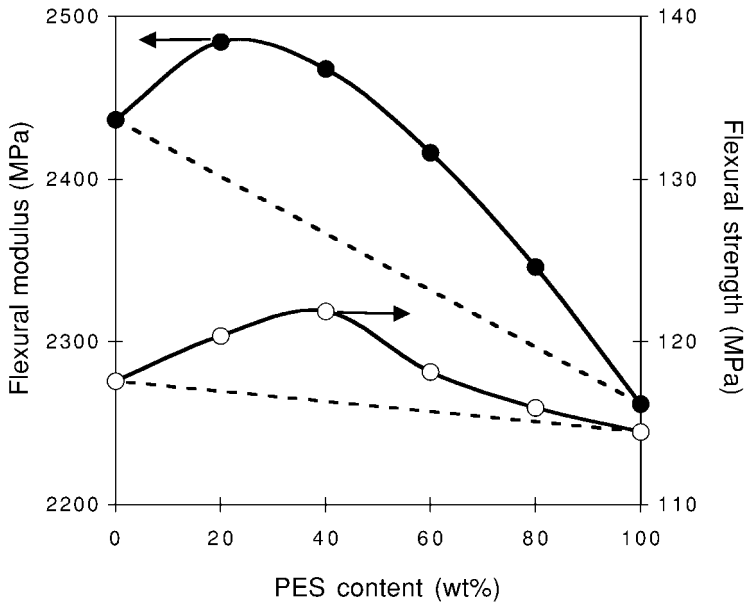

Figure 1 Flexural properties [(○) flexural strength; (●) flexural modulus] of N-TPI/PES blends.

ing perpendicularly to the melt-flow direction are shown in Figure 1. The flexural moduli and strength of the blends are greater than the arithmetic average of the moduli and the strength of the two pure components over the whole composition range. Especially, the strength and the moduli showed the highest values at a PES content of 40 and 20 wt %, respectively. Such a synergistic effect on the mechanical properties were reported on the blends containing LCP, for example, the blend of poly(butylene terephthalate) and LCP based on *p*-hydroxybenzoic acid (PHB) and poly(ethylene terephthalate) (Rodlan LC-3000)[9] and the blend of poly(ether ether ketone) and LCP based on PHB and 6-hydroxy-2-naphthoic acid (Vectra A950).[10] The synergism is attributed to the reinforcement by the fibrillation of LCP. The appearance of the remarkable synergism for the phase-separated blends without LCP, such as the N-TPI/PES blends, is thought to be a rare case. Regarding the miscible blends without LCP, it is known that the volume contraction due to a specific interaction gives rise to some synergism.[13]

To clarify the reasons why the synergistic effect on the flexural properties of the N-TPI/PES blends appears, the miscibility, crystallinity, and morphologies of the blends were investigated by the DSC and SEM measurements. Figure 2 shows the DSC thermograms of N-TPI, PES, and the N-TPI/PES (60/40) blend on the second heating DSC scans. The pure N-TPI and PES showed T_g's at 249 and 223°C, respectively. The T_g values of the N-TPI/PES blends of all the studied compositions are summarized in Table I. The N-TPI/PES blends over the whole composition range showed two T_g's (245–249°C and 221–226°C) corresponding to the N-TPI and PES components, indicating that the blends are an immscible system.

Figure 3 shows the first heating DSC thermogram of the injection-molded N-TPI. The N-TPI

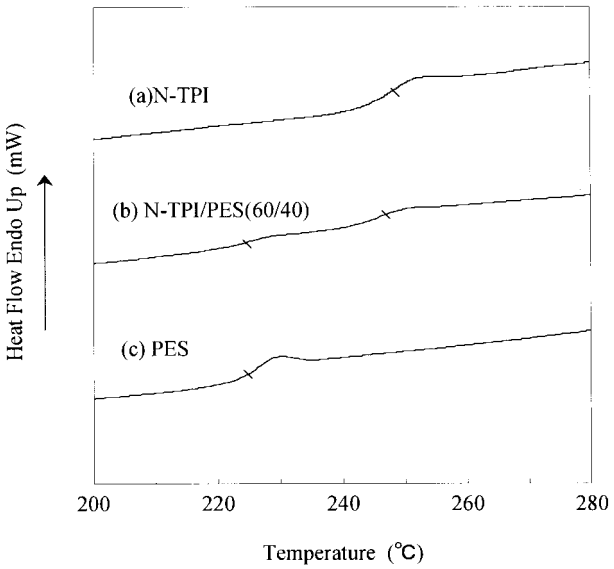

Figure 2 DSC thermograms of (a) N-TPI, (b) N-TPI/PES(60/40), and (c) PES on the second heating scans.

Table I Glass Transition Temperatures of the N-TPI/PES Blends

N-TPI/PES (Weight Ratio)	T_g (°C) PES Component	T_g (°C) N-TPI Component
0/100	223.3	—
20/80	221.0	248.9
40/60	225.6	246.0
60/40	223.4	246.7
80/20	225.6	245.0
100/0	—	249.3

sample showed an exothermal peak around 325°C due to crystallization and an endothermal peak around 380°C due to melting. The latter heat (ΔH_{m1}) minus the former heat (ΔH_{c1}) is, in principle, equal to the heat of melting of the crystalline region originally presented in the injection-molded sample. Therefore, the original degree of crystallinity [$\chi_{c0(\text{N-TPI})}$] normalized by the N-TPI weight fraction ($w_{\text{N-TPI}}$) for the injection-molded blend can be calculated by using the following equation:

$$\chi_{c0(\text{N-TPI})} = 100(\Delta H_{m1} - \Delta H_{c1})/(\Delta H_m^0 w_{\text{N-TPI}}) \quad (2)$$

where ΔH_{m1} and ΔH_{c1} are the heat of melting and crystallization of the blend in the first heating DSC scan, respectively, and ΔH_m^0 is the heat of melting of 100% crystalline N-TPI ($\Delta H_m^0 = 139.4$ J/g).[14] The values of ΔH_{m1}, ΔH_{c1}, and $\chi_{c0(\text{N-TPI})}$ of the blends are summarized in Table II. The original crystallinity of the injection-molded samples is very low (0.4–1.4%) irrespective to the composition, probably because the molding temperature is too low (120°C) to promote the crystallization of N-TPI. This result suggests that the influence of crystallinity on the flexural properties of the injection-molded samples is little.

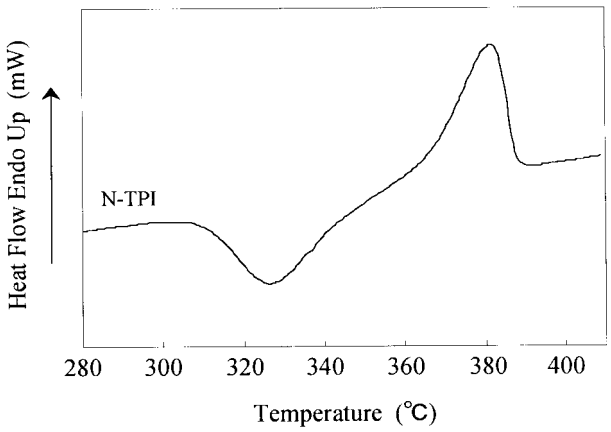

Figure 3 DSC thermogram of the injection-molded N-TPI on the first heating scan.

Table II Calorimetric Data and Crystallinity of the Injection-molded N-TPI/PES Blends

N-TPI Content (wt %)	ΔH_{c1} (J/g)	ΔH_{m1} (J/g)	$\chi_{c0(\text{N-TPI})}$ (%)
100	28.33	28.93	0.43
80	23.81	25.28	1.32
60	19.06	19.55	0.59
40	10.85	11.53	1.23
20	5.90	5.94	0.14

Figure 4 shows SEM micrographs of the cross section perpendicular to the melt-flow direction for the injection-molded blends. All the blends appeared phase-separated, in agreement with the result of the DSC measurement. It appeared that the dispersed phase is PES for the N-TPI/PES 80/20 and 60/40 blends and N-TPI for the 40/60 and 20/80 blends. The averaged diameter of the dispersed phase for the blend with the dispersed phase content of 20 wt % was smaller than that of 40 wt % content. Especially for the N-TPI/PES 80/20 blends, microphase separation (ca. 0.3 μm) of the dispersed PES phase was observed.

Figure 5 shows SEM micrographs of the cross section parallel to the melt-flow direction for the injection-molded N-TPI/PES blends. The PES fibers oriented along the flow direction appeared in both the skin and core regions of the N-TPI/PES 80/20 and 60/40 blends. For the N-TPI/PES 40/60 and 20/80 blends, the fibrillation of the N-TPI was observed only in the skin region, and the N-TPI phase in the core region was spherically dispersed. The appearance of synergism of the mechanical properties for the N-TPI/PES blends with a PES content higher than about 50 wt % is attributable to the reinforcement of the PES matrix by the fibrous N-TPI phase. For the N-TPI/PES blends with a PES content lower than about 50wt %, it is not expected that the less rigid PES fibers strengthen the rigid N-TPI matrix. From the SEM micrographs of Figure 5(a,b), it appears that the matrix of the N-TPI phase, in addition to the PES fiber, is more or less oriented along

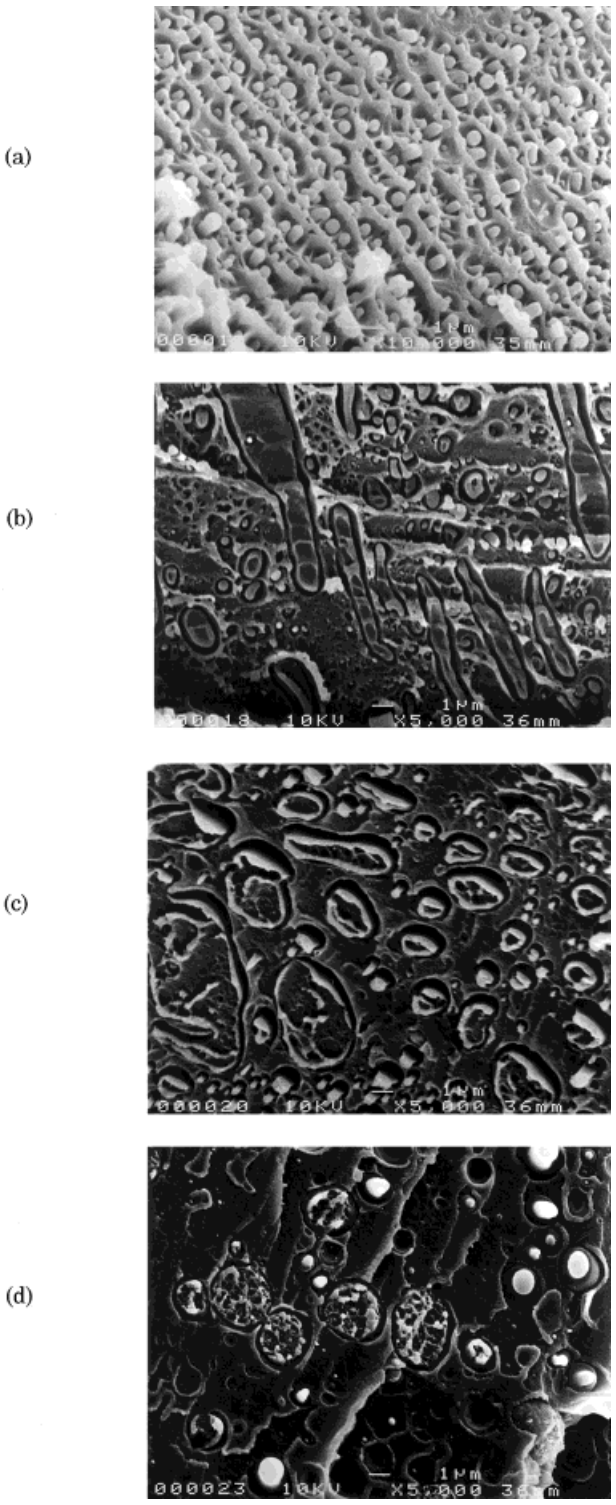

Figure 4 SEM micrographs of the cross section perpendicular to the melt-flow direction for the N-TPI/PES [(a) 80/20; (b) 60/40; (c) 40/60; (d) 20/80] blends.

the melt-flow direction. The orientation of N-TPI molecules may contribute to the improvement of the flexural properties.

Crystallization Behavior of the N-TPI/PES Blends

The injection-molded samples of the N-TPI/PES blend had low crystallinity. Although we tried annealing the molded sample at 250–350°C, the dumbbell specimen became deformed due to the softening of the PES component. To obtain a specimen with high crystallinity, the molding temperature should be first held at around the crystallization temperature of N-TPI (300–350°C) and, subsequently, cooled down to a temperature lower than the T_g of PES (223°C). The crystallization behavior of the semicrystalline polymer is found to be highly influenced by the presence of the second components such as inorganic or organic fillers and other thermoplastics.[15–17] To obtain information on the crystallization behavior of N-TPI blended with PES and the ultimate crystallinity after holding at a crystallization temperature for a very long time, the isothermal crystallization behavior of the N-TPI/PES (100/0–60/40) blends over a temperature range of 315–330°C was monitored by DSC measurement. Figure 6 shows a typical isothermal crystallization scan of the blends at 320°C. The isothermal crystallization kinetics of the blends was analyzed using the Avrami equation:

$$\chi_c(t)/\chi_c(\infty) = 1 - \exp(-kt^n) \qquad (3)$$

where k is the rate constant of crystallization and n is the Avrami exponent, which can be related to the type of nucleation and to the geometry of crystal growth. From the intercepts and the slopes of the plots of $\log\{-\ln[1 - \chi_c(t)/\chi_c(\infty)]\}$ versus $\log t$ (example plot at T_c of 325°C , Fig. 7), the values of k and n were calculated, respectively; all these values are summarized in Table III. Each curve has a linear portion followed by a gentle roll-off at longer times. With decrease of the PES content (especially 0 and 10 wt %), the change of slope was observed at a shorter time. In this case, the slope at the shorter crystallization time corresponding to primary crystallization was adopted. The values of the Avrami exponent n (2.0–3.0) of the N-TPI/PES (90/10–60/40) blends increased with increasing PES content. Regarding n for pure N-TPI, the value obtained in this study was 2.22–2.33, in agreement with the values (2.0–2.2) reported by Torre et al.[14] for the isothermal crystallization at a T_c of 290–360°C. The crystallization half-times, $t_{1/2}$, the time at which the relative degree of crystallization is 0.5, increase with increasing PES content. The rate

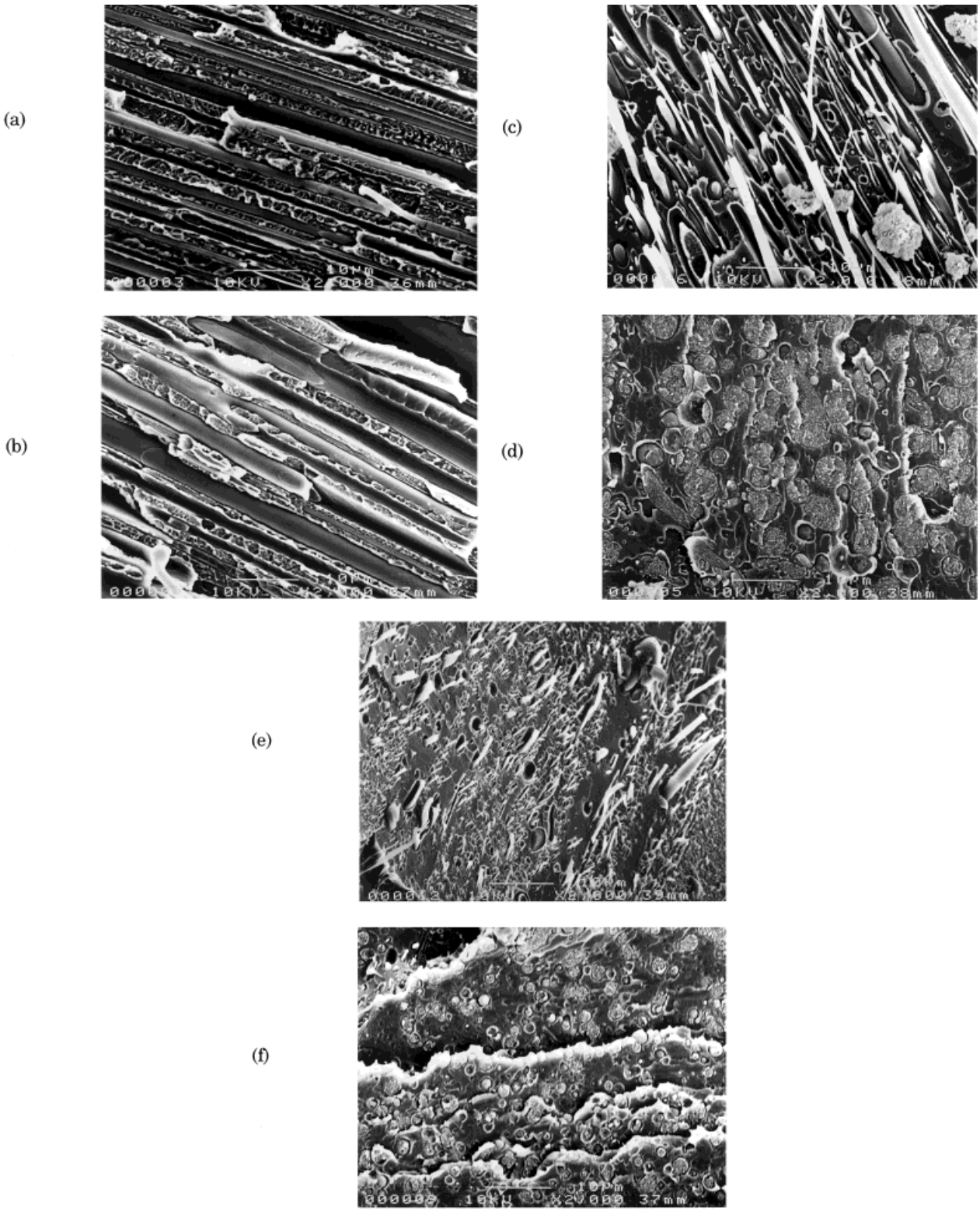

Figure 5 SEM micrographs of the cross section parallel to the melt-flow direction for the N-TPI/PES [(a) 80/20; (b) 60/40; (c) 40/60 (skin region); (d) 40/60 (core region); (e) 20/80(skin region); (f) 20/80 (core region)] blends.

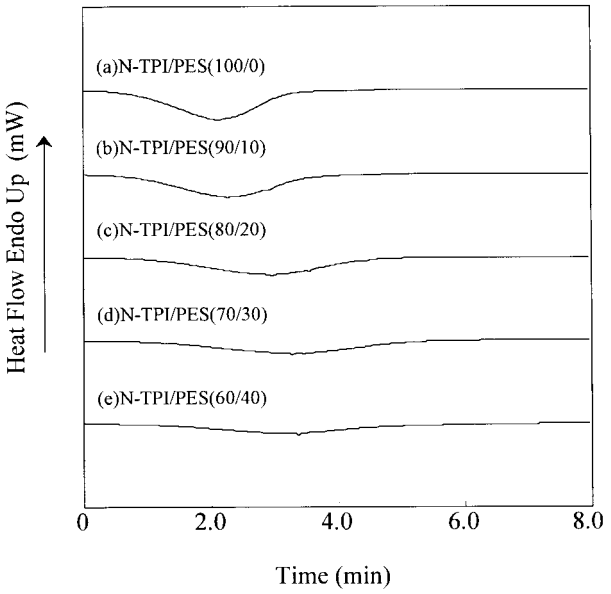

Figure 6 Typical DSC isothermal crystallization curves of the N-TPI/PES blends at 320°C.

constant decreased with increasing PES content except for the case of a PES content of 10 wt %. The rate constant in the primary crystallization process of the N-TPI/PES 90/10 blend was the highest for all the T_c studied.

According to Hoffman–Weeks theory,[18] the dependence of the apparent melting temperature

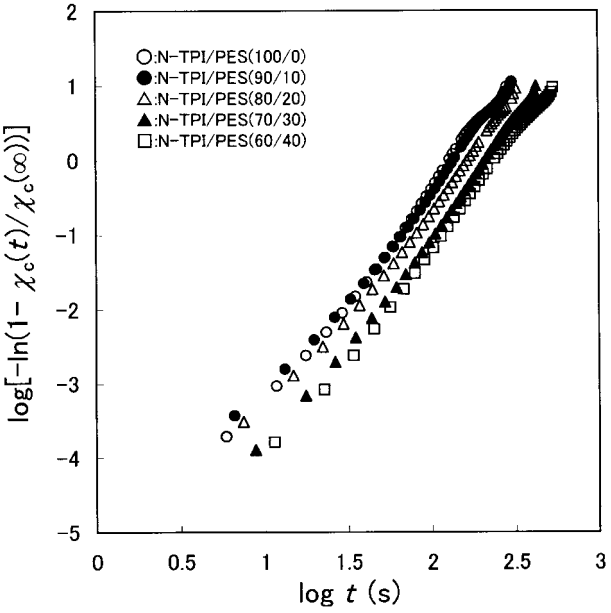

Figure 7 Example plots of $\log\{-\ln[1 - \chi_c(t)/\chi_c(\infty)]\}$ versus $\log t$ for N-TPI/PES blends at T_c of 325°C.

Table III Isothermal Crystallization Parameters for N-TPI in the Blends with PES

T_c (°C)	N-TPI/PES	$t_{1/2}$ (s)	k (s^{-n})	n
315	100/0	129	3.52×10^{-6}	2.29
	90/10	147	6.91×10^{-6}	2.04
	80/20	168	1.38×10^{-6}	2.27
	70/30	179	1.26×10^{-7}	2.77
	60/40	203	1.21×10^{-7}	2.98
320	100/0	122	4.07×10^{-6}	2.22
	90/10	136	7.45×10^{-6}	2.01
	80/20	168	1.95×10^{-6}	2.14
	70/30	190	1.28×10^{-7}	2.77
	60/40	175	1.26×10^{-7}	2.96
325	100/0	116	3.08×10^{-6}	2.33
	90/10	135	5.90×10^{-6}	2.18
	80/20	162	3.27×10^{-6}	2.23
	70/30	188	2.83×10^{-7}	2.56
	60/40	210	1.21×10^{-7}	2.58
330	100/0	126	1.77×10^{-6}	2.33
	90/10	145	5.53×10^{-6}	2.02
	80/20	162	8.18×10^{-7}	2.31
	70/30	193	6.21×10^{-7}	2.53
	60/40	205	3.50×10^{-7}	2.58

(T_m) on the crystallization temperature (T_c) is given by

$$T_m = (1 - 1/\gamma)T_m^0 + (1/\gamma)T_c \quad (4)$$

where T_m^0 is the equilibium melting point and γ is the lamellar thickening factor which describes the growth of lamellar thickness during crystallization. Therefore, from the extrapolation of the melting point versus the T_c curve to its intersection with the line $T_m = T_c$, T_m^0 can be estimated. The melting temperature observed at the heating scan after isothermal crystallization was plotted against T_c for N-TPI/PES (100/0–60/40) blends (example plot of 80/20 blend, Fig. 8). The obtained T_m^0's are summarized in Table IV. The T_m^0 of pure N-TPI was 391°C, which value is relatively close to the literature values of N-TPI of 399°C reported by Torre et al.[14] The obtained T_m^0 for the blends (389–393°C) was little affected by the presence of PES.

The normalized degree of crystallinity [$\chi_{c(\text{N-TPI})}$] of the isothermally crystallized blend can be estimated from the DSC results by using the following equation:

$$\chi_{c(\text{N-TPI})} = 100\Delta H_{m2}/(\Delta H_m^0 w_{\text{N-TPI}}) \quad (5)$$

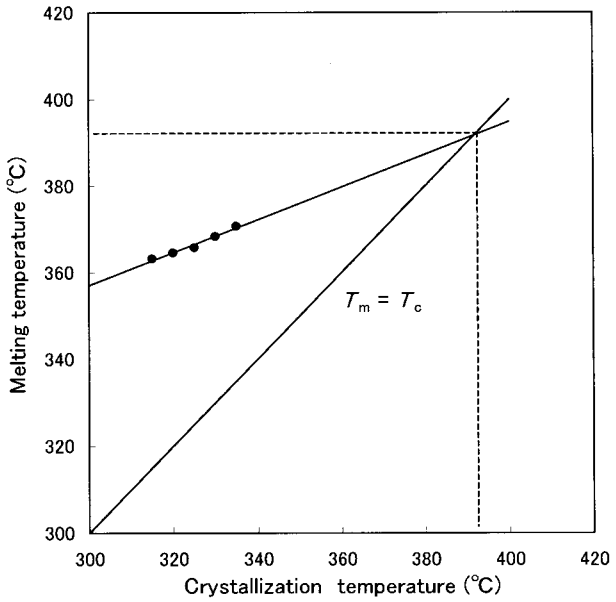

Figure 8 Hoffman–Weeks plots to determine the equilibrium melting temperature of N-TPI with PES content of 20 wt %.

where ΔH_{m2} is the heat of melting on the heating DSC scan after isothermal melt crystallization of the blend. The crystallinity data are given in Table IV. The $\chi_{c(\text{N-TPI})}$ values at the PES content of 10 wt % was higher than those of pure N-TPI. The $\chi_{c(\text{N-TPI})}$ values of the blends with the PES content higher than 10 wt % was lower than those of pure N-TPI for all the T_c studied. In the case of melt crystallization at 315–330°C of the blends, both the rate constant and degree of crystallinity of the N-TPI component for the blend with the PES content of 10 wt % are higher than are those of pure N-TPI. The reason is not clear, but it is thought that the mobility of the N-TPI segment increases by the addition of PES because PES has a lower T_g than that of N-TPI. Actually, for the N-TPI/PES (90/10) blend, the T_g of the N-TPI rich phase is 243°C, which is a little lower than the T_g of pure N-TPI (249°C). However, the former T_g does not decrease with an increasing PES content, as shown in Table I, because N-TPI and PES are immiscible. Therefore, further addition of PES to N-TPI does not contribute to increase of the mobility of N-TPI molecules but results in decrease of the N-TPI concentration.

CONCLUSIONS

The flexural moduli and strength of the injection-molded N-TPI/PES blends are greater than is the arithmetic average of the moduli and strength of the two pure components over the whole composition range. The DSC measurement revealed that the blend is an immiscible system and that the crystallinity of the N-TPI component is very low (0.4–1.4%) irrespective of the composition. The SEM analysis suggested that the improve-

Table IV Parameters Related to the Fusion of the Crystalline Formed by Isothermal Melt Crystalliztion of the N-TPI/PES Blends

	T_c (°C)				
Blends	315	320	325	330	T_m^0 (°C)
N-TPI/PES = 100/0					391.2
ΔH_{m2} (J/g)	25.6	24.8	25.7	25.4	
$\chi_{c(\text{N-TPI})}$ (wt %)	18.1	17.8	18.5	18.2	
N-TPI/PES = 90/10					389.5
ΔH_{m2} (J/g)	22.8	23.3	25.5	26.0	
$\chi_{c(\text{N-TPI})}$ (wt %)	18.2	18.6	20.4	20.8	
N-TPI/PES = 80/20					391.8
ΔH (J/g)	16.0	17.3	15.1	16.1	
$\chi_{c(\text{N-TPI})}$ (wt %)	14.3	15.5	13.6	14.5	
N-TPI/PES = 70/30					392.6
ΔH_{m2} (J/g)	13.4	14.8	16.8	14.1	
$\chi_{c(\text{N-TPI})}$ (wt %)	13.7	15.2	17.3	14.5	
N-TPI/PES = 60/40					392.2
ΔH_{m2} (J/g)	12.0	12.7	11.6	11.8	
$\chi_{c(\text{N-TPI})}$ (wt %)	14.4	15.1	13.9	14.1	

ment in the flexural properties is likely due to the reinforcement of the PES matrix by the fibrous N-TPI phase for the PES-rich blends. For the N-TPI-rich blends, the orientation of the matrix N-TPI rather than the fibrillation of the PES phase along the melt-flow direction may contribute to the synergism observed. Also, the study on the isothermal crystallization behavior of the blends revealed that the addition of 10 wt % PES accelerates the crystallization of N-TPI and causes a slight increase of the ultimate crystallinity.

REFERENCES

1. Technical data sheet/A00: NEW-TPI, Mitsui–Toatsu Co.
2. Hou, T. H.; Reddy, J. M. Sampe Q 1991, 22, 38.
3. Huo, P. P.; Friler, J. B.; Cebe, P. Polymer 1993, 34, 4387.
4. Friler, J. B.; Cebe, P. Polym Eng Sci 1993, 33, 587.
5. Huo, P. P.; Cebe, P. Polymer 1993, 34, 696.
6. Ma, S. P.; Takahashi, T. Polymer 1996, 25, 5589.
7. Furukawa, H.; Morita, A.; Koba, T. Polym Prepr Jpn 1993, 42, 3917.
8. Sauer, B. B.; Hsiao, B. S. Polymer 1993, 34, 3315.
9. Sun, L.-M.; Sakoda, T.; Ueta, S.; Koga, K. Takayanagi, M. Polym J 1994, 26, 961.
10. Mahta, A.; Isayev, A. I. Polym Eng. Sci 1991, 31, 971.
11. Jang, S. H.; Kim, B. S. Polym Eng. Sci 1994, 34, 847.
12. Akhtar, S.; Isayev, A. I. Polym Eng Sci 1993, 33, 32.
13. MacKnight, W. J.; Karasz, F. E.; Fried, J. R. In Polymer Blends; Paul, D. R.; Newman, S., Eds.; Academic: London, 1978; Chapter 5.
14. Torre, L.; Maffezzoli, A.; Kenny, J. M. J Appl Polym Sci 1995, 56, 985.
15. Shingankuli, V. L; Jog, J. P. Nadkarni, V. M. J Appl Polym Sci 1988, 36, 335.
16. Benjamim, D.; Bretas, R. E. S. J Appl Polym Sci 1995, 55, 233.
17. Shibata, M.; Yosomiya, R.; Jiang, Z.; Yang, Z.; Wang, G.; Ma, R.; Wu, Z. J Appl Polym Sci 1999, 74, 1686.
18. Hoffman, J. D.; Weeks, J. J. J Chem Phys 1962, 37, 1723.